PERGAMON

International Journal of Solids and Structures 39 (2002) 6411–6427

INTERNATIONAL JOURNAL OF SOLIDS and STRUCTURES

www.elsevier.com/locate/ijsolstr

Large-scale testing of space steel frame subjected to non-proportional loads

Seung-Eock Kim *, Kyung-Won Kang

Department of Civil and Environmental Engineering/Construction Tech. Research Institute, Sejong University, 98 Koonja-dong, Kwangjin-ku, Seoul 143-747, South Korea

Received 22 June 2001; received in revised form 25 July 2002

Abstract

This paper presents large-scale testing of a space steel frame. Considering a majority of large-scale frame tests in the past, only two-dimensional frames are experimentally studied. Therefore, three-dimensional experiment is needed to extend the knowledge of this field. A two-story, single-bay, and sway allowed frame subjected to non-proportional vertical and horizontal load was tested. Details of the test frame, test instruments, set-up and test procedures and the load–displacement curve of the test frame are presented. The experimental results are useful in the verification of three-dimensional analytical models. Non-linear numerical analysis was also performed, and its results compared well with the experimental results. It was observed that the load carrying capacity calculated by the AISC-LRFD method was 28% conservative when compared with that by the experiment. This difference is attributed to the fact that the AISC-LRFD approach does not consider the inelastic moment redistribution but the experiment includes the inelastic redistribution effect.

Keywords: Non-linear inelastic analysis; Ultimate strength; Space steel frame; Buckling; Yielding

1. Introduction

The second-order inelastic analysis enables designers to directly evaluate the ultimate strength and behavior of structural system. The direct use of second-order inelastic analysis without member capacity checks is expected to be allowed in future design codes. Over the past 30 years, researchers have developed and validated various methods of performing second-order inelastic analysis on steel frames. Most of these studies can be categorized into one of two types: sophisticated and simplified second-order inelastic analysis. The sophisticated analysis (plastic-zone analysis) uses the highest refinement and is considered accurate (Clarke et al., 1992; Vogel, 1985). However, this analysis is not intended to be used in daily

* Corresponding author. Tel.: +82-2-3408-3291; fax: +82-2-3408-3332.
E-mail address: sekim@sejong.ac.kr (S.-E. Kim).

0020-7683/02/$ - see front matter © 2002 Elsevier Science Ltd. All rights reserved.
PII: S0020-7683(02)00463-8

engineering practice, because it is too costly and intensive in computation. The simplified analysis for practical design uses the concentrated plastic hinge (Kim et al., 2002; Kim et al., 2001; Kim and Choi, 2001; Liew et al., 2000; Chen and Kim, 1997). This analysis must be verified by calibrating with plastic-zone analysis. The plastic-zone analysis also requires an experimental verification in order to confirm its validity, since experimental results provide actual behavior and strength of structures. Therefore, a realistic simulation such as large-scale frame testing is quite necessary.

Two-dimensional two-bay full-size frames were tested by Kanchanalai (1977) to verify the plastic-zone analysis. All frames were bent with respect to the weak axis in order to avoid out-of-plane buckling. Two-dimensional full-size frames were tested by Yarimci (1966) at Lehigh University. The frames were sandwiched and supported laterally by two parallel auxiliary frames preventing out-of-plane buckling. All members were bent about the strong axis. A series of four tests was conducted by Avery and Mahendran (2000). Each of the four frames could be classified as a two-dimensional, single-bay, single-story, large-scale sway frame with full lateral restraint and rigid joints. Two-series of test were conducted by Wakabayashi and Matsui (1972) for a two-dimensional one-story frame and a two-story frame. To prevent out-of-plane buckling, two of the same specimens were set in parallel and connected at the joints and at the mid-length of the members. Harrison (1964) tested the equilateral triangular space frame. A horizontal load (H) was applied on the top of the column and a vertical load of 1.3H was applied at mid-span of the beam.

Although many large-scale frame tests have been conducted in the past 30 years, the majority of them are of only two-dimensional frames. Two-dimensional frames are not a realistic representative model of the behavior of real structures. The aim of this paper is to conduct three-dimensional large-scale frame testing.

2. Test frames

The steel frame tested could be classified as a large-scale three-dimensional, two-story, one-bay, rigidly jointed, and sway frame.

2.1. Dimensions

The dimensions of the test frame were 2.5 m wide in X-direction, 3 m long in Y-direction, 1.76 m high from the column base to the second floor, and 2.2 m high from the second floor to the roof. Fig. 1 shows the dimensions of the test frame. The frame was designed to fail by the combined effects of yielding and instability. The dimensions were carefully decided to avoid lateral torsional buckling of a single member. A failure by inelastic lateral torsional buckling of a single member would not be appropriate in investigating global behavior of combined yielding and second-order instability of the frame. The slenderness (L_c/r) of the column members of the first and the second floors were 25 and 32 about strong axis and 43 and 55 about weak axis, respectively, which were representative of typical structures.

2.2. Three-dimensional frame

Many common steel frame tests in the past were performed with simplified two-dimensional assemblages for ease of testing, even though the real structures were three-dimensional. It is obvious that two-dimensional test has difficulty in simulating three-dimensional behavior including space torsion. Therefore, test frame presented in this paper was three-dimensional. Figs. 2 and 3 show a schematic three-dimensional drawing and a photograph of the test frame.

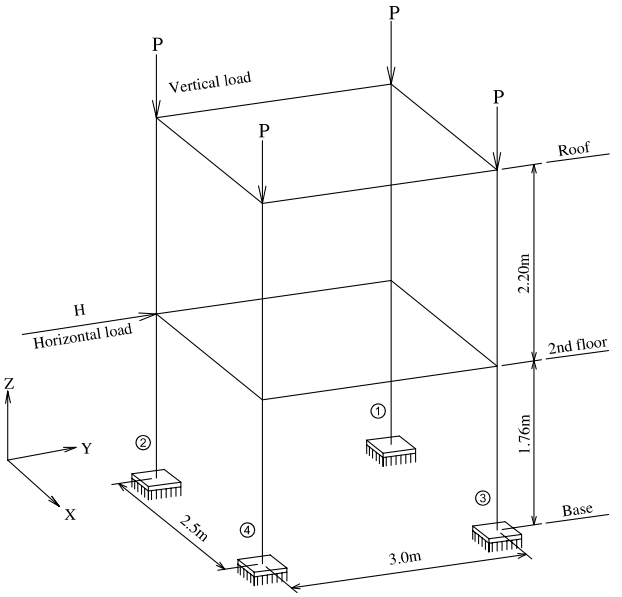

Fig. 1. Dimensions and loading conditions of test frame in main test.

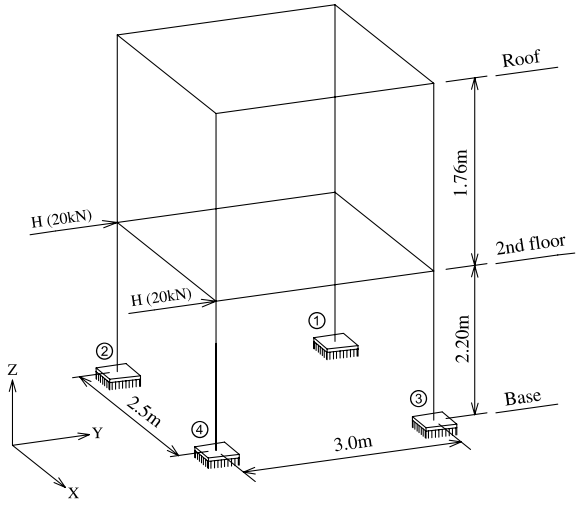

Fig. 2. Loading conditions of test frame in pre-test.

2.3. Sway frame

A sway frame was selected since the stability of sway frames is more complex than that of non-sway frames. The stability of sway frames involves both $P-\Delta$ and $P-\delta$ effects, while that of non-sway frames deals only with $P-\delta$ effects.

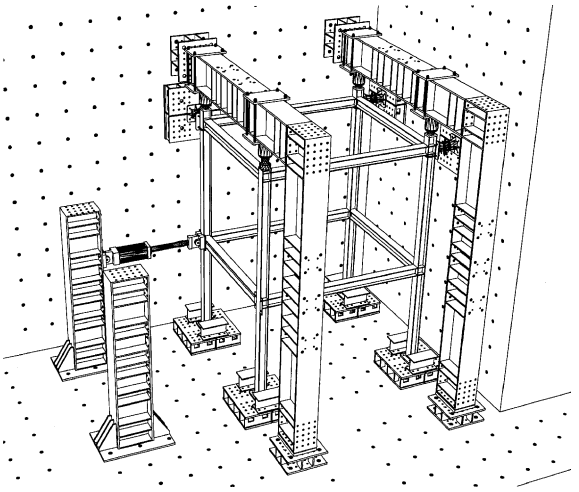

Fig. 3. Schematic drawing of test arrangement in main test.

2.4. Two-story and single-bay frame

Previous experimental studies were conducted often for one-story single-bay or sometimes for two-story single-bay frames. A two-story, single-bay frame was chosen in this study. The main reason for selecting a two-story frame is its convenience in including $P-\Delta$ effect in the test frame without moving the horizontal positions of vertical jacks. Since the same structural principles are used for both two-story, single-bay and more complex multi-story, multi-bay structures, the two-story, single-bay frame was enough to investigate structural behavior.

2.5. Structural connections

Structural connections, in general, can be classified as rigid, pinned, or semi-rigid. Rigid connection was used in the test frame. The beam to column connections were fully welded to make rigid connection. Column base connections were made as rigid as possible. The base plate of 30 mm thickness was continuously fillet welded to the column. Each base plate was fastened to the heavily reinforced base block using four M24 bolts with the center-to-center distance of 200 mm. Fig. 4 shows the connection of the column base.

2.6. Section

Hot-rolled wide flange section was used for the test frame. Nominal dimension of the section was H-$150 \times 150 \times 7 \times 10$ commonly used in Korea. The dimensions and properties of the section are listed in Table 1. The section is compact so that it is not susceptible to local buckling. Failure by elastic and inelastic local buckling of a single member would not be appropriate in investigating global behavior of the test frame.

2.7. Material

Material used was grade SS400 steel with nominal yield stress of 250 MPa, commonly used in Korea.

Fig. 4. Column base connection and dial gauge.

Table 1
Dimensions and properties of section H-150 × 150 × 7 × 10 used in the frame

		Height H (mm)	Width B (mm)	Thickness of flange t_f (mm)	Thickness of web t_w (mm)	Radius of fillet r_1 (mm)	Gross area A_g (mm^2)	Moment of inertia about X-axis I_X (10^6 mm^4)	Moment of inertia about Y-axis I_Y (10^6 mm^4)
Nominal		150	150	10	7	11	4014	16.40	5.63
Measured	Column	152.3	149.9	10.2	6.75	–	4053	17.20	5.74
	Beam	149.1	150.0	9.2	6.50	–	3713	15.14	5.18

3. Test instrument

3.1. General

The frame was tested in the strong floor, wall, and loading frame which could sustain 2000 kN. The strong floor and wall were 1.0 and 2.0 m thick, respectively. The three-dimensional schematic drawing and photograph of the test set-up are shown in Figs. 2 and 3, respectively. The test facilities were in the structural engineering laboratory of the Institute of Technology of Hyundai Construction Company.

3.2. Loading frame

The height from the strong floor surface to the top of the loading frame was 5.45 m and the distance from the shear wall surface to the inner face of the loading frame column was 4.4 m. The column base of the loading frame was fastened with 16 M24 bolts to the heavily reinforced base block, which was fastened again with four M50 bolts to the strong floor. The one end of the girder of the loading frame was fastened with 16 M24 bolts to the base block, which was bolted again with four M50 bolts to the strong wall. The other end of the girder was fastened with 16 M24 bolts to the column. The girder and column depth and width of the loading frame were 0.6 and 0.4 m, respectively. The flange and web thickness were 25 and 20 mm, respectively.

3.3. Hydraulic jack

Four 1000 kN hydraulic jacks with 100 mm stroke were mounted at the bottom flange of the loading frame girder in alignment with the center of each of the four columns of the test specimen so that the vertical loads could be applied to the columns without eccentricity. The four vertical jacks were connected by one pump so that they could produce equal loads simultaneously. A 1000 kN load cell was installed between the hydraulic jack and the top of Column ④. A single load cell was enough to measure the applied loads, since the hydraulic jacks generated equal loads. Figs. 5 and 6 show the four vertical jacks and the load cell.

30 mm thick steel plate was welded to transfer the vertical jack forces to the flange and web of Columns ①, ②, and ③ without local crushing of the column web. A thinner plate of 20 mm was used for Column ④

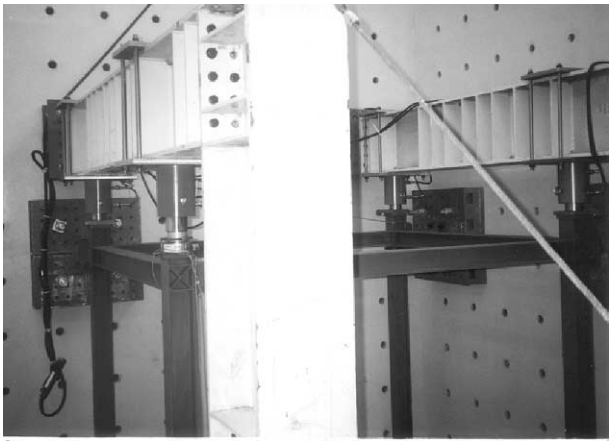

Fig. 5. Four vertical jacks and load cell.

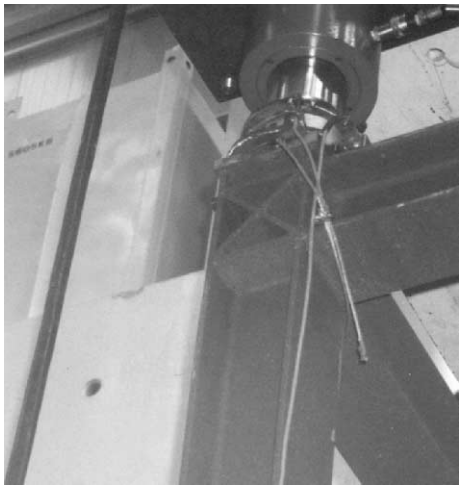

Fig. 6. Load cell on Column ④.

since the load cell diameter placed on the top of Column ④ was 150 mm which was bigger than the piston diameter of 125 mm of the hydraulic jack.

3.4. Actuator

Two actuators were installed on the flanges of the loading columns at the height of 2.03 m from the strong floor surface. Two actuators were used during pre-test while one actuator was used in the main-test. The sectional dimensions of the loading columns were identical with those of the loading frame members. The bases of the loading columns were fastened with six M50 bolts to the strong floor. The actuators generated horizontal loads applied at the second floor level of the test frame. The actuators allow shortening of the columns since they have the hinge at the both ends of the piston.

3.5. Boundary conditions of test frame

The test frame was semi-fixed in displacement and rotation at the base level, free to move at the second floor level, and fixed in displacement at the roof level. The base plates of the four columns of the test frame were fastened with four M24 bolts to the heavily reinforced base block, which was fastened again with four M50 bolts to the strong floor.

The horizontal displacements of the test frame at the roof level were restrained by the three screw-jack supports, which were bolted to the base block on the wall. Thus, the vertical jack force was applied concentrically to the top of the column. The load cell on Column ④ allows rotation. Special devices under the vertical jacks for Column ①–③ were not used so that ideal free rotation conditions could not be achieved. The restraint on rotation, however, was not regarded significant since the piston diameter was only 125 mm. Fig. 7 shows the screw-jack support. The reason to use the screw-jack is that it can easily touch the frame face by screwing after installation of the test frame regardless of the magnitude of fabrication error. The small convex shape steel plate was welded to the front face of the screw-jack in order to minimize friction force. As a result, the screw-jack restrains horizontal displacement but not vertical displacement. The screw-jack is shown in Fig. 8.

An U-bolt was installed at each screw-jack as shown in Fig. 7. The U-bolt binded the column just below the bottom flange of the beam, and restrained the in-plane rotation about the Z-axis of the roof level. The purpose of this U-bolt was to prevent any unwanted horizontal movement in opposite direction to the

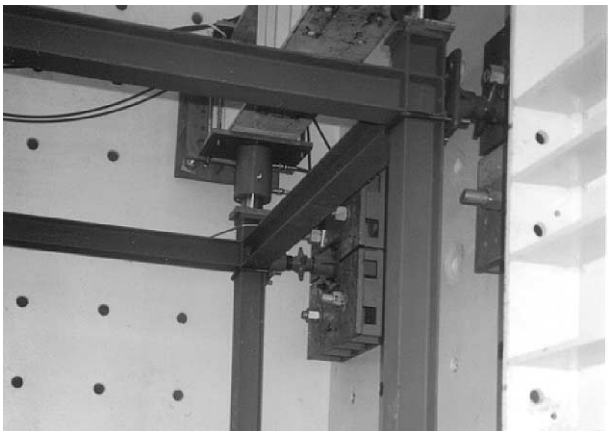

Fig. 7. Screw-jack support and U-bolt.

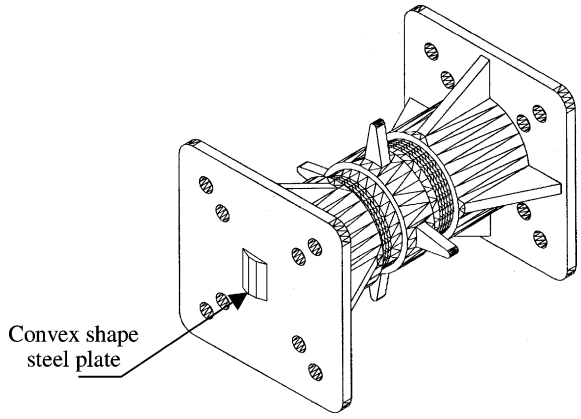

Fig. 8. Screw-jack.

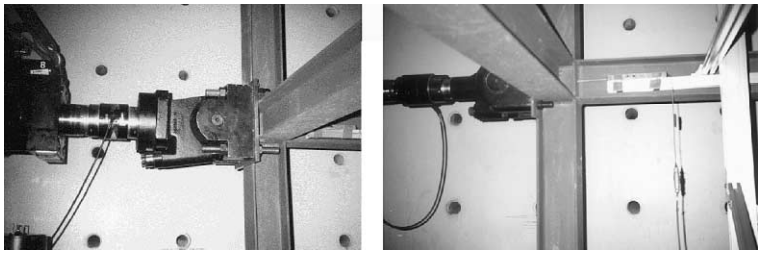

Fig. 9. Horizontal actuator and LVDT at second floor level.

strong walls under the vertical loads. The U-bolt, however, did not restrain the rotation (with respect to the X-axis) generated as the test frame deformed, since the applied horizontal load caused the horizontal displacement in the direction toward the strong walls at the level of the U-bolt.

3.6. Instrument of measurement

The actuator would measure the horizontal displacements caused not only at the test frame but also at the loading column. Linear variable differential transformers (LVDTs) were installed at the second floor level to measure the real horizontal displacement at Columns ② and ④ of the test frame. Fig. 9 shows the actuator and the corresponding LVDT. LVDT was installed to check the horizontal slip of the base plate as shown in Fig. 4. The electric signals from the two LVDTs, two actuators, and one load cell were fed directly into a data acquisition system which was connected again to the computer system, closely monitoring the behavior of the test frame during the test.

4. Test procedure and results

4.1. Material test

Stress–strain curves were obtained by tensile testing. The tensile testing was conducted in accordance with the Korean standard KS B 0801. The measured dimensions of the beam members were different from

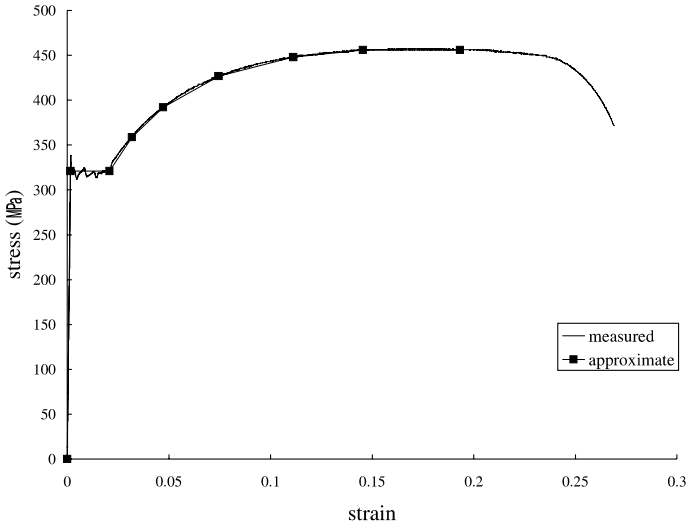

Fig. 10. Stress–strain curve for H-150 × 150 × 7 × 10 steel (flange of the column).

Table 2
Multi-linear stress–strain curves for H-150 × 150 × 7 × 10 steel

Column	Flange	Stress (MPa)	0	320	320	360	388	426	446	453	455
		Strain	0	0.00147	0.02190	0.03375	0.04708	0.07450	0.11123	0.14548	0.19320
	Web	Stress (MPa)	0	311	311	367	408	436	445	442	–
		Strain	0	0.00145	0.02063	0.04230	0.07055	0.11640	0.16485	0.21863	–
Beam	Flange	Stress (MPa)	0	344	344	397	434	455	463	464	–
		Strain	0	0.00155	0.02190	0.04708	0.07450	0.11123	0.14548	0.19320	–
	Web	Stress (MPa)	0	327	327	366	406	435	445	443	–
		Strain	0	0.00168	0.02063	0.04230	0.07055	0.11640	0.16485	0.21863	–

those of the column members as listed in Table 1, although the nominal dimensions of the beam and column members were identical as H-150 × 150 × 7 × 10. Four specimens were tested. Each specimen was taken from the flange and web of the beam and column members, respectively. The stress–strain curve obtained from the tensile testing of the specimen taken from the flange of the column is shown in Fig. 10. The stress–strain curve was of typical shape for mild steel with a short elastic region and a long yield plateau followed by a significant long strain hardening region. The strain hardening started at the strain range from 0.02 to 0.03. The unloading occurred at the strain range of 0.2–0.25. The specimens had higher yield stresses ranging from 310 to 350 MPa than the nominal yield stress of 250 MPa. The ultimate stress of the specimens was approximately 450 MPa which was within the range of the nominal ultimate stress of 400–510 MPa. The approximate multi-linear curve is added in Fig. 10 and their coordinates at each point are listed in Table 2.

4.2. Pre-test

Although the column base was intended to be rigidly connected, the rigidly bolted connection cannot be achieved in real situation. The pre-test was conducted to evaluate the flexibility of the bolted connection of the column base. For the pre-test, no restraint was provided at the roof level in order to make boundary

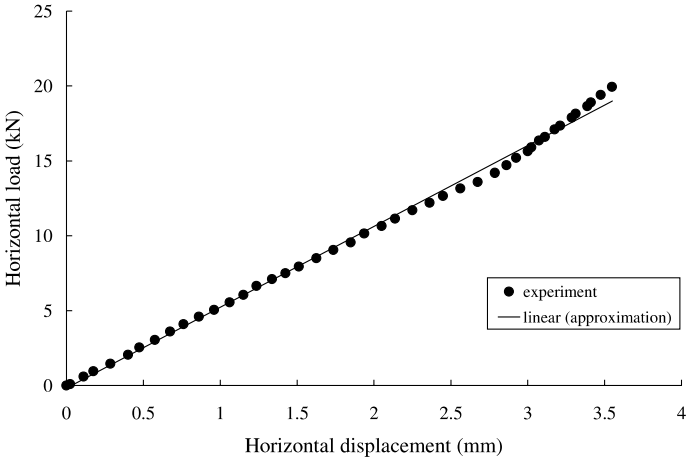

Fig. 11. Horizontal load–displacement curve of the pre-test (Column ②).

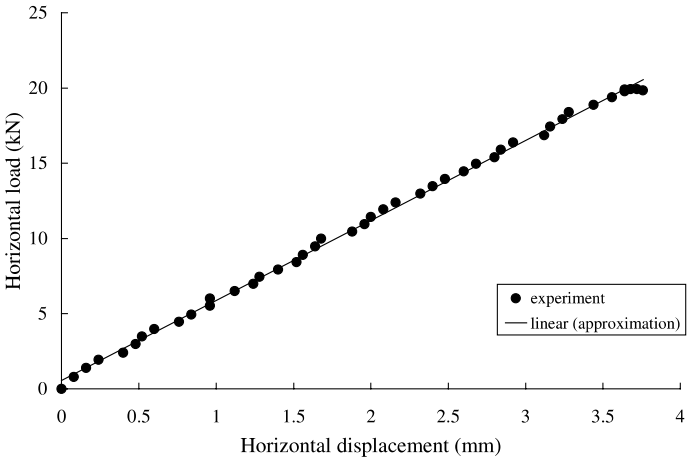

Fig. 12. Horizontal load–displacement curve of the pre-test (Column ④).

condition as simple as possible. Two actuators applied identical horizontal loads on Columns ② and ④ of the test frame (Fig. 2).

The horizontal load was increased up to 20 kN so that the test frame will remain within an elastic range. The LVDT measured the horizontal displacements at Columns ② and ④ at the second floor level. The load–displacement relationship is illustrated in Figs. 11 and 12. The horizontal displacement was used to determine the connection flexibility at the column base.

4.3. Measurement of imperfections

The out-of-plumbness of the columns in X- and Y-directions was measured using an electro-optical system. The out-of-straightness was not measured since it did not make significant difference to the behavior of unbraced frames. The local imperfections were ignored since the used frame section was compact and not governed by local buckling. The measured out-of-plumbness was summarized in Table 3.

Table 3
Measured out-of-plumbness imperfections

Level	Imperfections (mm)							
	Column ①		Column ②		Column ③		Column ④	
	X	*Y*	*X*	*Y*	*X*	*Y*	*X*	*Y*
Roof	−1.6	−6.8	2.91	−3.5	13.5	−10.7	−3.84	−7.21
Second floor	2.8	−3.1	−0.3	−2.4	11.89	−8.43	−3.39	−4.95
Base	0	0	0	0	0	0	0	0

A positive imperfection indicates that the column was offset in the positive direction in the X and Y axes shown in Fig. 1.

4.4. Main test

The vertical loads were applied to the top of the four columns, and the horizontal load was applied to Column ② at the second floor level of the test frame (Fig. 3). The reason to use one horizontal load is to

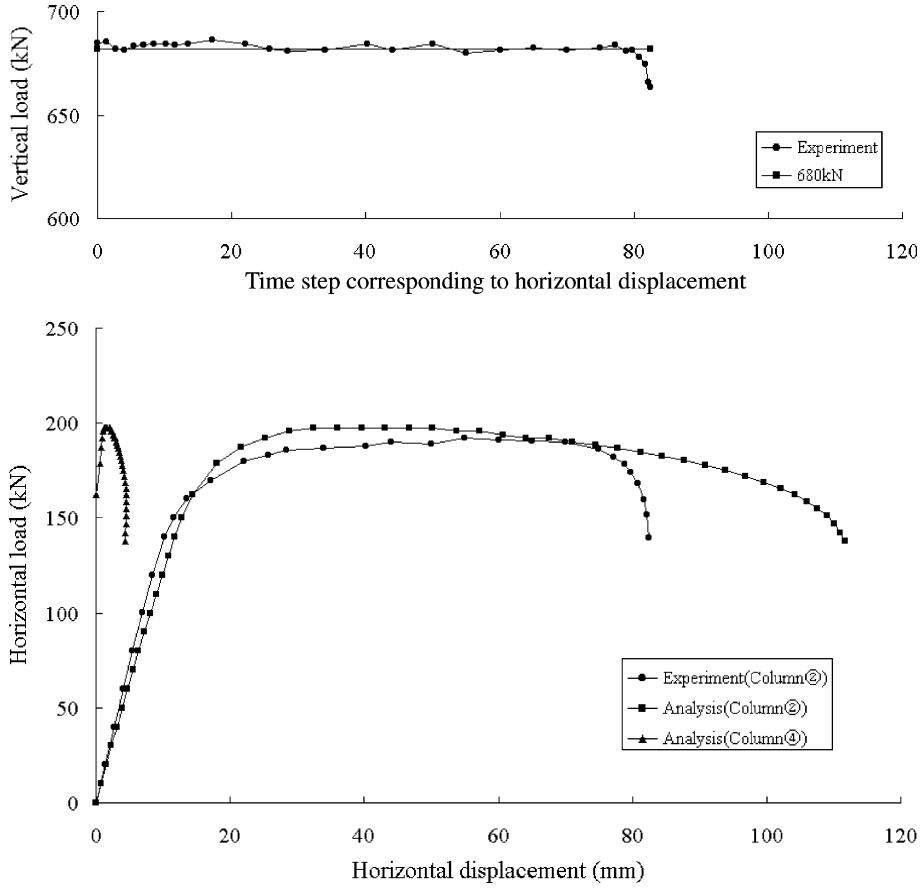

Fig. 13. Horizontal load–displacement curve for test frame (Column ②).

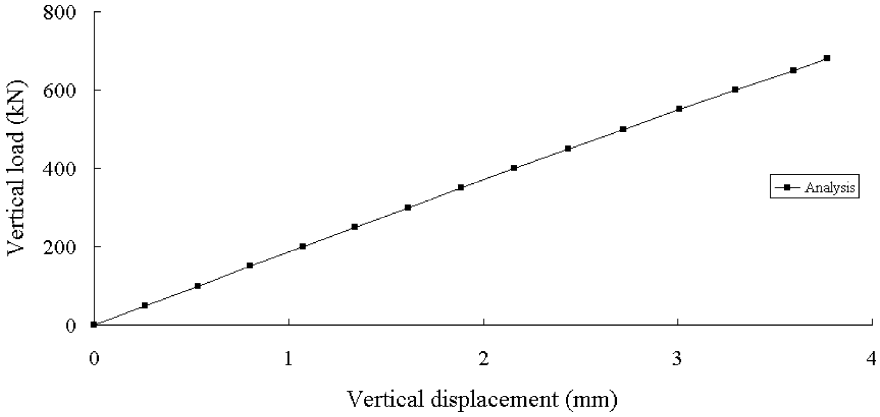

Fig. 14. Vertical load–displacement curve for test frame (Column ②).

Table 4
Comparison of experimental and design load carrying capacities

	(a) Experiment	(b) Analysis	(c) AISC-LRFD design	(b)/(a)	(c)/(a)
P	612.0	612.0	443.5	1.0000	0.7247
H	169.2	175.5	122.6	1.0372	0.7246

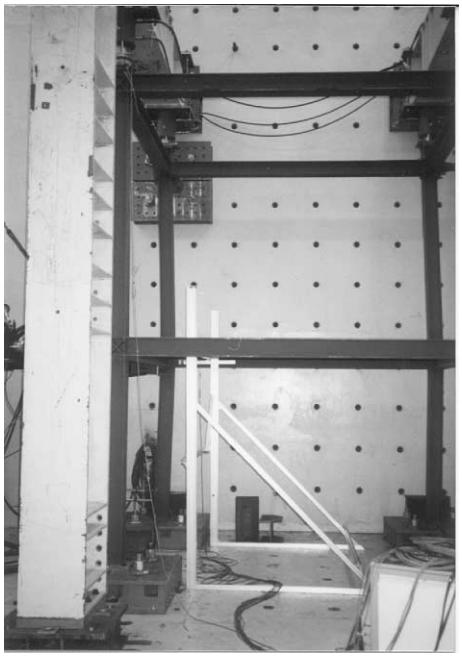

Fig. 15. Deflected shape of test frame at ultimate state.

obtain more dominant spatial behavior including global torsion. The displacement-controlled test was performed in Main test in order to trace the descending branch in the load–displacement curve. The vertical loads were first increased 680 kN equivalent to 0.53Py and maintained during the experiment. Py is the squash load of the column section H-150 × 150 × 7 × 10. The target vertical load was 0.6Py but the maximum working capacity of the vertical jack was 680 kN. The horizontal displacement was slowly increased until the test frame could not resist any more loads. The time required to finish test was approximately 30 min. The LVDT measured the horizontal displacement of Column ② at the second floor level. The load–displacement curves are illustrated in Figs. 13 and 14. The curve can be used to verify numerical analysis results. The load carrying capacity of test frame is listed in Table 4. The load carrying capacity indicates the maximum load that the test frame can sustain. The frame failed by instability due to $P-\Delta$ moment, coupled with reduced stiffness due to yielding. The deflected shape of the test frame at ultimate state is shown in Fig. 15.

5. Numerical analysis

A 3-D non-linear analysis was performed using ABAQUS, one of the mostly widely used and accepted commercial finite element analysis program. ABAQUS S4R and STRI35 shell elements were used for the analysis of test frame models (Fig. 16). Eight elements through the depth of the web and across the width of the flange were used (Fig. 17). An aspect ratio close to unity was used in the direction of flange width and web depth. The base plate connection was simulated by horizontal and vertical springs used at 25 nodal points. The spring constants were varied in the numerical model of pre-test frame until the analytical and experimental results agreed. The horizontal and vertical spring constants attached at 25 nodal points of the base plate were determined as 67,322 kN/m. The horizontal and vertical spring constants were assumed identical due to limited data obtained by pre-test. The multi-linear stress–strain curves listed in Table 2 were used for the analysis of the test frame. The measured elastic moduli and yield stresses listed in Table 5 were used. Poisson's ratio used was 0.3.

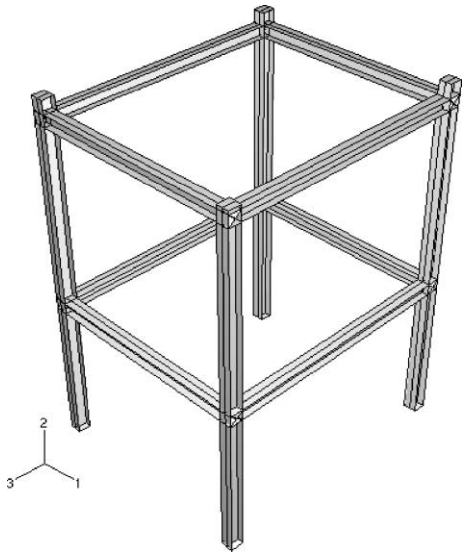

Fig. 16. 3-D finite element modeling.

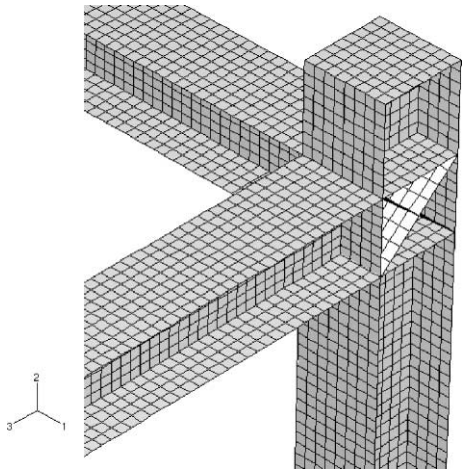

Fig. 17. Finite element mesh.

Table 5
Yield stress and elastic modulus

		Yield stress (MPa)	Ultimate stress (MPa)	Elastic modulus (MPa)
Column	Flange	320	455	217,771
	Web	311	442	214,504
Beam	Flange	344	464	221,313
	Web	327	443	194,814

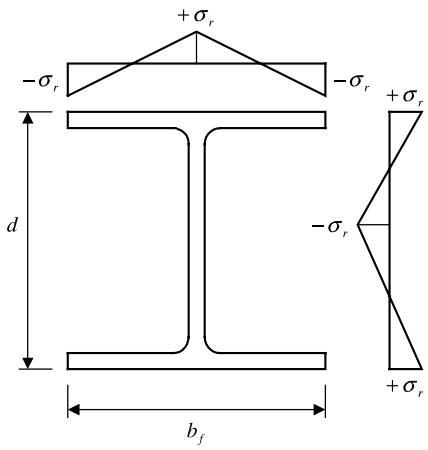

Fig. 18. Assumed longitudinal membrane residual stress distribution for hot-rolled I-sections.

Out-of-plumbness imperfections were explicitly modeled. The magnitude of the measured imperfections in the test frames was used (Table 3). Out-of-straightness imperfections were not included since $P-\delta$ effects are not dominant in unbraced frames. Local imperfections were not modeled since the test frame was comprised of compact sections. The longitudinal membrane residual stress distributions recommended by

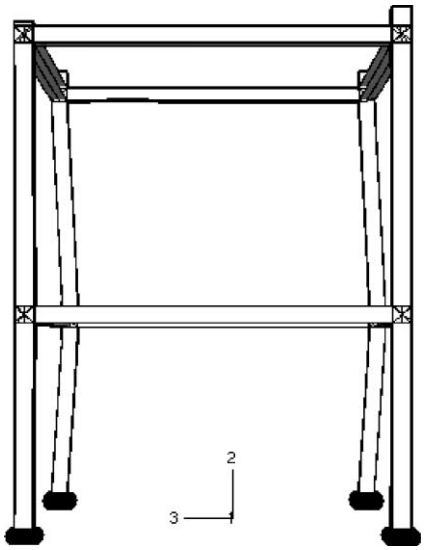

Fig. 19. Deflected shape at ultimate state of test frame.

ECCS Technical Committee 8 (1984) was adopted (Fig. 18). The maximum residual stress was selected as 50% of the yield stress. The residual stress distributions were modeled using ABAQUS *INITIAL CONDITIONS option. The initial stresses were defined using the SIGINI FORTRAN user subroutine (Kim and Lee, 2002). These subroutines define the local components of the initial stress as a function of the element number.

The vertical concentrated nodal forces representing the vertical jack loads were applied at the top of each column without eccentricity. Horizontal nodal displacements simulating the horizontal jack loads were applied concentrically to the outside flange of Column ② at the second floor level (Fig. 1).

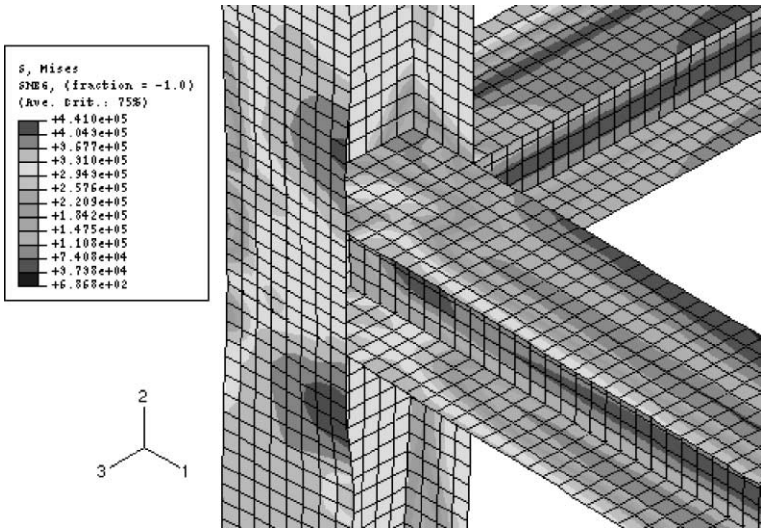

Fig. 20. Stress distribution at second floor level of Column ②.

Geometric and material non-linear static analysis was performed to obtain the ultimate load carrying capacity. The arc-length method with the minimum time increment of 10^{-5} was used for non-linear analyses. The horizontal load deflection curves obtained from the analysis of the test frame is compared with the experimental curve in Fig. 13. The ultimate load obtained from the non-linear analysis and experiment are nearly the same within 3.7% difference as shown in Table 4. The horizontal displacements obtained from the experiment and the analysis show little difference. This difference can be attributed to possible experimental errors (i.e., boundary conditions, eccentric loading, variations in the material properties, and residual stresses) and analytical approximations (i.e., nominal residual stresses, imperfection distributions, and simplified stress–strain curves). Deflected shape at the final step of numerical analysis is shown in Fig. 19. It can be observed that large deflection occurs at Column ②. Stress distribution at second floor level of Column ② is shown in Fig. 20. Stress concentration occurs at the area of the beam-to-column connection.

6. Comparison of test result with AISC-LRFD capacity

Load carrying capacities obtained from the experiment, analysis, and AISC-LRFD method are compared in Table 4. The AISC-LRFD capacity was obtained using the average measured yield stresses of the flange and web specimens. A resistance factor of 0.9 was used in the experiment and analysis capacity, while factors of 0.85 for columns and 0.9 for beams were used in the AISC-LRFD capacity. The results showed that the AISC-LRFD capacity was approximately 28% conservative. This difference is derived from the fact that the AISC-LRFD approach does not consider the inelastic moment redistribution, but the experiment and analysis include the inelastic redistribution effect. This comparison provides concrete reasons to use an inelastic non-linear analysis which is quite necessary to reduce member sizes. It is important to note that the conventional design approach using semi-empirical specification equations for separate member capacity checks after linear elastic analysis of a structural system should be replaced by advanced analysis, i.e., inelastic non-linear analysis in the near future.

7. Conclusions

This paper has presented details of large-scale testing of space steel frames in order to provide benchmarking data. Considering the majority of large-scale frame tests in the past, only two-dimensional frames are experimentally studied. Therefore, this three-dimensional experiment can be regarded quite valuable. The test frame was carefully designed to fail by combined effects of yielding and instability rather than inelastic lateral torsional buckling of a single member. The pre-test was conducted to evaluate the flexibility of the bolted connection of the column base.

The load–displacement curve of the test frame is provided. The experimental results are useful for verification of three-dimensional analytical models. The ultimate load obtained from the experiment and non-linear analysis agreed well within 3.7%. The horizontal displacement between the experiment and the analysis shows little difference. This is attributed to possible experimental errors and analytical approximations. The load carrying capacity calculated by the AISC-LRFD method was 28% conservative compared with the experimental results. This difference is derived from the fact that the AISC-LRFD approach does not consider the inelastic moment redistribution but the experiment includes the inelastic redistribution effect.

Acknowledgements

This work presented in this paper was supported by funds of National Research Laboratory Program (grant no. 2000-N-NL-01-C-162) from Ministry of Science and Technology in Korea. Authors wish to appreciate the financial support.

References

Avery, P., Mahendran, M., 2000. Large-scale testing of steel frame structures comprising non-compact sections. Eng. Struct. 22, 920–936.

Chen, W.F., Kim, S.E., 1997. LRFD Steel Design Using Advanced Analysis. CRC Press, Boca Raton, Florida.

Clarke, M.J., Bridge, R.Q., Hancock, G.J., Trahair, N.S., 1992. Benchmarking and verification of second-order elastic and inelastic frame analysis programs. In: White, D.W., Chen, W.F. (Eds.), SSRC TG 29 Workshop and Monograph on Plastic Hinge Based Methods for Advanced Analysis and Design of Steel Frames. SSRC, Lehigh University, Bethlehem, PA.

ECCS 1984. Ultimate limit state calculation of sway frames with rigid joints. Technical Committee 8-Structural Stability Technical Working Group 8.2-System. Publication no. 33. European Convention for Constructional Steelwork.

Harrison, H.B., 1964. The Application of the principles of plastic analysis to three dimensional steel structures. Ph.D. thesis, Department of Civil Engineering, University of Sydney.

Kanchanalai, T., 1977. The design and behavior of beam-columns in unbraced steel frames. AISI Project no. 189, Report no. 2, Civil Engineering/Structures Research Lab., University of Texas, Austin, p. 300.

Kim, S.E., Choi, S.H., 2001. Practical advanced analysis for semi-rigid space frames. Solids Struct. 38, 9111–9131.

Kim, S.E., Lee, D.H., 2002. Second-order distributed plasticity analysis of space steel frames. Eng. Struct. 24, 735–744.

Kim, S.E., Park, M.H., Choi, S.H., 2001. Direct design of three-dimensional frames using practical advanced analysis. Eng. Struct. 23, 1491–1502.

Kim, S.E., Lee, J.H., Park, J.S., 2002. 3-D second-order plastic-hinge analysis accounting for lateral torsional buckling. Solids Struct. 39, 2109–2128.

Liew, R.J.Y., Chen, H., Shanmugam, N.E., Chen, W.F., 2000. Improved nonlinear plastic hinge analysis of space frame structures. Eng. Struct. 22, 1324–1338.

Vogel, U., 1985. Calibrating frames. Stahlbau 10, 1–7.

Wakabayashi, M., Matsui, C., 1972. Elastic–plastic behaviors of full size steel frame. Trans. Arch. Inst. Jpn. 198, 7–17.

Yarimci, E., 1966. Incremental inelastic analysis of framed structures and some experimental verification. Ph.D. dissertation, Department of Civil Engineering, Lehigh University, Bethlehem, PA.